Sensor fault detection for rail vehicle suspension systems with disturbances and stochastic noises

Zehui Mao, Yanhao Zhan, Gang Tao, *Fellow, IEEE*, Bin Jiang, *Senior Member, IEEE*, Xing-Gang Yan

***Abstract*—This paper develops a sensor fault detection scheme for rail vehicle passive suspension systems, using a fault detection observer, in the presence of uncertain track regularity and vehicle noises which are modeled as external disturbances and stochastic process signals. To design the fault detection observer, the suspension system states are augmented with the disturbances treated as new states, leading to an augmented and singular system with stochastic noises. Using system output measurements, the observer is designed to generate the needed residual signal for fault detection. Existence conditions for observer design are analyzed and illustrated. In term of the residual signal, both fault detection threshold and fault detectability condition are obtained, to form a systematic detection algorithm. Simulation results on a realistic vehicle system model are presented to illustrate the observer behavior and fault detection performance.**

***Index Terms*—Fault detection, observer design, rail vehicle suspension systems.**

I. Introduction

Suspension systems for rail vehicles are used to support the carbody and bogie, to isolate the road-induced vibrations, and to control the vertical and angular of the carbody with respect to the track surface to provide the comfortable services to passengers. The suspension systems can be classified into three categories: passive suspension system (built with spring and damper); semi-active suspension system (built with spring and variable damper) and active suspension system (built with spring, damper and actuator). Since the suspension system is an essential part for vehicles, different controllers have been proposed and tested on these kinds of suspension systems, see [1], [2], [3] and [4]. Similar to the other practical systems, the faults in sensors, actuators (in active suspension systems) or process (plant) of the suspension systems may drastically change the system behavior, resulting in performance degradation or even instability. Therefore, effective fault detection technologies are crucial for the suspension systems.

This work was supported in part by the National Natural Science Foundation of China under Grant 61573180, Grant 61374130,and Grant 61490703).

Z. Mao and B. Jiang are with College of Automation Engineering, Nanjing University of Aeronautics and Astronautics, Nanjing, 210016, China, Email: zehuimao@nuaa.edu.cn (Z. Mao), binjiang@nuaa.edu.cn (B. Jiang).

Z. Zhan is with CRRC Zhuzhou Institute Co., Ltd, Zhuzhou, 412001, China, Email: guangjiao@nuaa.edu.cn, and he has done this work when he was a graduate student in College of Automation Engineering, Nanjing University of Aeronautics and Astronautics.

G. Tao is with Department of Electrical and Computer Engineering, University of Virginia, Charlottesville, VA 22904, U.S.A, and he is a visiting professor in the Nanjing University of Aeronautics and Astronautics, Email: gt9s@virginia.edu (corresponding author).

X. Yan is with School of Engineering and Digital Arts, University of Kent, Canterbury, Kent CT2 7NT, United Kingdom, Email: x.yan@kent.ac.uk.

Fault detection (FD) and diagnosis have been investigated for several years, and many results are available in several books [5]-[7] and many papers [8]-[13]. A widely used method for fault detection is the model-based observer or filter design method. When the plant models are available, the method could be effective and independent of the history dates that the date-driven method needs. And some existing observer design methods could be extended to achieve the fault detection, such as [14]-[16]. For suspension systems, the motion models have been well studied and many results have been obtained, see [1], [2] and [3]. On the other hand, the track irregularity is a key and non-ignore element for rail vehicle suspension systems. One main task for suspension systems is to reduce the forces generated by the track unevenness. This motivates many researchers to study the fault problems for suspension systems in the presence of the disturbances/uncertainties or noises. The popular method to this problem is to design the robust residuals, such that the effect of the exogenous disturbance on the residuals is attenuated with respect to a minimized H_2/H_∞ norm, see [17]-[20]. Moreover, the index between the residual and fault is required to guarantee that the sensitivity of the residual to the fault is enhanced by means of a maximized H_2/H_∞ norm, see [21], [22] and [23]. This method can be used to deal with a class of uncertainties, which are bounded by functions of energy. However, the corresponding robust and sensitivity residual generation method to deal with stochastic noises, is unavailable in the existing literature. Thus, one of the motivations for this paper is that the fault detection problem for suspension systems in the presence of the disturbances and stochastic noises is not fully studied.

Although the fault problem for active suspension systems is a hot research topic, (see e.g. [24], [25] and [26]), in reality, passive suspension systems are widely used in rail train, due to their simple structure, low cost, and non-power requirement to achieve the ride performance and quality. The needs to monitor the states of the passive suspension systems and to design the controller for active suspension systems, make the sensors to be important equipments. Note that most of the existing work for fault detection is about the actuator or process (plant) faults, in which the sensor fault detections are rarely studied. However, sensor faults widely exist in the real world. It is worth studying the fault detection problems for sensors faults.

This paper is focused on the sensor fault detection for the passive vehicle suspension systems with disturbances and stochastic noises. A fault detection observer is proposed such that the state and unknown external disturbances (track irregularity) are estimated simultaneously to generate the residual. The thresholds are chosen with enhanced fault detection rates

for the suspension systems with stochastic noise. The main contributions of this paper are as follows: (i) The unknown external disturbances and process noises, which can affect the fault residual performance and can not be ignored for the suspension system, with sensor faults, are considered in this approach. To deal with the disturbances, an augmented system is introduced to transform the original system to a singular system with stochastic noises. (ii) A fault detection observer is designed for the new singular system to estimate the system disturbances and generate the residual. Further the existence conditions of the presented observer are also developed for general suspension systems. (iii) Based on the analysis of the residual and the stochastic noises, necessary conditions for the fault detection are given, which facilitate to obtain the false and missing alarm rates.

The rest of the paper is organized as follows: Section 2 describes the suspension system model. Section 3 studies a fault detection observer with existence conditions. Sections 4 proposes the fault detection decision scheme. Section 5 includes the simulation study, followed by conclusions in Section 6.

II. Suspension model with disturbances and faults

The suspension mechanism adopted for the rail vehicles is shown in Figure 1.

Fig. 1: Multibody dynamic platform of the rail vehicle

According to the references [2], [3], [26], and the equipment used in companies, the passive suspension system mechanism adopted, can be shown in Figure 2, which consists of two power cars (car 1 and car 3) and a trailer car (car 2) with carbody and bogie, respectively. The passive force of the secondary suspension between the carbody and bogie is dependent on their relative displacement. The articulation is always simulated as a spring. There are nine sensors mounted on the suspension systems to obtain the associated data. The bounce and pitch motions of its carbodies and the bounce motions of its bogies should be the main focus. It is important to note that if the pitch motion of the bogie is also considered here, extra 3 DOFs (degree of freedoms) are required for system modelling to describe the pitch angle, which makes the study more complex and is unnecessary. Therefore, the pitch angle of the bogie is ignored here in order to convenient.

In Figure 2, y_1, y_2 and y_3 are the vertical displacements of the center of gravity of the first power carbody, the trailer

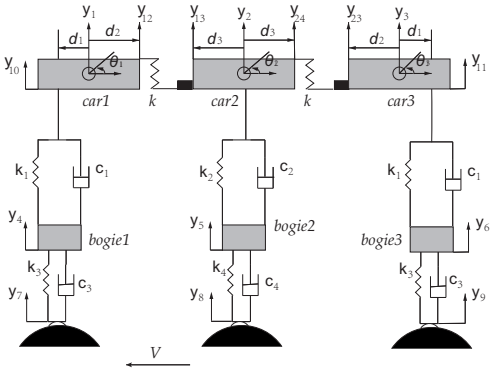

Fig. 2: Suspension systems of the rail vehicle

carbody and the second power carbody; θ_1, θ_2 and θ_3 are the pitch angles of the first power carbody, the trailer carbody and the second power carbody; y_4, y_5 and y_6 are the vertical displacements of the first power bogie, the trailer bogie and the second power bogie; y_7, y_8 and y_9 are the track vertical profiles (track irregularity) for the first power bogie, the trailer bogie and the second power bogie.

A. Continuous-time model with disturbances and faults

The continuous state-space model of the above suspension system dynamics (see [3]) can be written in the continuous state-space model format as (see [1], [3], [26]):

$$\dot{x}(t) = A'x(t) + B'g(x,t) + D'd(t) + \delta'(t) \tag{1}$$
$$z(t) = Cx(t) + F_s f(t) + \eta(t) \tag{2}$$

where A', B', $g(\cdot,\cdot)$, C, D' and F_s are state-space matrix, input matrix and nonlinear function, output matrix, disturbance and fault distributing matrix, respectively.

$$A' = \begin{bmatrix} A'_{11} & A'_{12} & A'_{13} \\ A'_{21} & A'_{22} & A'_{23} \\ A'_{31} & A'_{32} & A'_{33} \end{bmatrix}, \quad B' = \begin{bmatrix} B'_{11} & B'_{12} & B'_{13} \\ B'_{21} & B'_{22} & B'_{23} \\ B'_{31} & B'_{32} & B'_{33} \end{bmatrix},$$

$$D' = \begin{bmatrix} D'_1 & 0 & 0 \\ 0 & D'_2 & 0 \\ 0 & 0 & D'_3 \end{bmatrix}, \quad C = \begin{bmatrix} C_1 & 0 & 0 \\ 0 & C_2 & 0 \\ 0 & 0 & C_3 \end{bmatrix}$$

$$A'_{11} = \begin{bmatrix} \frac{-c_1}{m_p} & \frac{c_1 d_1}{m_p} & \frac{c_1}{m_p} & -\frac{k_1+k}{m_p} & 0 & \frac{k_1}{m_p} \\ \frac{c_1 d_1}{I_p} & -\frac{c_1 d_1^2}{I_p} & -\frac{c_1 d_1}{I_p} & \frac{k_1 d_1 - k d_2}{I_p} & 0 & -\frac{k_1 d_1}{I_p} \\ \frac{c_1}{m_{pb}} & -\frac{c_1 d_1}{m_{pb}} & -\frac{c_1+c_3}{m_{pb}} & \frac{k_1}{m_{pb}} & 0 & \frac{k_1+k_3}{m_p} \\ 1 & 0 & 0 & 0 & 0 & 0 \\ 0 & 1 & 0 & 0 & 0 & 0 \\ 0 & 0 & 1 & 0 & 0 & 0 \end{bmatrix},$$

$$A'_{12} = \begin{bmatrix} 0 & 0 & 0 & \frac{k}{m_p} & 0 & 0 \\ 0 & 0 & 0 & \frac{k d_2}{I_p} & 0 & 0 \\ 0 & 0 & 0 & 0 & 0 & 0 \\ 0 & 0 & 0 & 0 & 0 & 0 \\ 0 & 0 & 0 & 0 & 0 & 0 \end{bmatrix}, \quad A'_{13} = 0_6, \quad A'_{21} = \begin{bmatrix} 0 & 0 & 0 & \frac{k}{m_t} & 0 & 0 \\ 0 & 0 & 0 & -\frac{k d_2}{I_t} & 0 & 0 \\ 0 & 0 & 0 & 0 & 0 & 0 \\ 0 & 0 & 0 & 0 & 0 & 0 \\ 0 & 0 & 0 & 0 & 0 & 0 \end{bmatrix},$$

$$A'_{22} = \begin{bmatrix} \frac{-c_2}{m_t} & 0 & \frac{c_2}{m_t} & -\frac{k_2+2k}{m_t} & 0 & \frac{k_2}{m_t} \\ 0 & 0 & 0 & 0 & 0 & 0 \\ \frac{c_2}{m_{tb}} & 0 & -\frac{c_2+c_4}{m_{tb}} & \frac{k_2}{m_{tb}} & 0 & -\frac{k_2+k_4}{m_{tb}} \\ 1 & 0 & 0 & 0 & 0 & 0 \\ 0 & 1 & 0 & 0 & 0 & 0 \\ 0 & 0 & 1 & 0 & 0 & 0 \end{bmatrix},$$

$$A'_{23}=\begin{bmatrix}0&0&0&\frac{k}{m_t}&0&0\\0&0&0&\frac{kd_3}{I_t}&0&0\\0&0&0&0&0&0\\0&0&0&0&0&0\\0&0&0&0&0&0\\0&0&0&0&0&0\end{bmatrix},\quad A'_{31}=0_6,\quad A'_{32}=\begin{bmatrix}0&0&0&\frac{k}{m_p}&0&0\\0&0&0&-\frac{kd_2}{I_p}&0&0\\0&0&0&0&0&0\\0&0&0&0&0&0\\0&0&0&0&0&0\\0&0&0&0&0&0\end{bmatrix},$$

$$A'_{33}=\begin{bmatrix}-\frac{c_1}{m_p}&-\frac{c_1d_1}{m_p}&\frac{c_1}{m_p}&-\frac{k_1+k}{m_p}&0&\frac{k_1}{m_p}\\-\frac{c_1d_1}{I_p}&-\frac{c_1d_1^2}{I_p}&\frac{c_1d_1}{I_p}&\frac{kd_2-k_1d_1}{I_p}&0&\frac{k_1d_1}{I_p}\\\frac{c_1}{m_{pb}}&\frac{c_1d_1}{m_{pb}}&-\frac{c_1+c_3}{m_{pb}}&\frac{k_1}{m_{pb}}&0&-\frac{k_1+k_3}{m_p}\\1&0&0&0&0&0\\0&1&0&0&0&0\\0&0&1&0&0&0\end{bmatrix},$$

$$B'_{11}=\begin{bmatrix}0&0&0&0&\frac{k_1d_1-kd_2}{m_p}&0\\0&0&0&0&-\frac{k_1d_1^2+kd_2^2}{I_p}&0\\0&0&0&0&-\frac{k_1d_1}{m_{pb}}&0\\0&0&0&0&0&0\\0&0&0&0&0&0\\0&0&0&0&0&0\end{bmatrix},\quad B'_{12}=\begin{bmatrix}0&0&0&0&-\frac{kd_3}{m_p}&0\\0&0&0&0&-\frac{kd_2d_3}{I_p}&0\\0&0&0&0&0&0\\0&0&0&0&0&0\\0&0&0&0&0&0\\0&0&0&0&0&0\end{bmatrix},$$

$$B'_{13}=O_6,\quad B'_{21}=\begin{bmatrix}0&0&0&0&\frac{kd_2}{m_t}&0\\0&0&0&0&-\frac{kd_2d_3}{I_t}&0\\0&0&0&0&0&0\\0&0&0&0&0&0\\0&0&0&0&0&0\\0&0&0&0&0&0\end{bmatrix},$$

$$B'_{22}=\begin{bmatrix}0&0&0&0&0&0\\0&0&0&0&-\frac{2kd_3^2}{I_t}&0\\0&0&0&0&0&0\\0&0&0&0&0&0\\0&0&0&0&0&0\\0&0&0&0&0&0\end{bmatrix},\quad B'_{23}=\begin{bmatrix}0&0&0&0&-\frac{kd_2}{m_t}&0\\0&0&0&0&-\frac{kd_2d_3}{I_t}&0\\0&0&0&0&0&0\\0&0&0&0&0&0\\0&0&0&0&0&0\\0&0&0&0&0&0\end{bmatrix},$$

$$B'_{31}=O_6,\quad B'_{32}=\begin{bmatrix}0&0&0&0&\frac{kd_3}{m_p}&0\\0&0&0&0&-\frac{kd_2d_3}{I_p}&0\\0&0&0&0&0&0\\0&0&0&0&0&0\\0&0&0&0&0&0\\0&0&0&0&0&0\end{bmatrix},$$

$$B'_{33}=\begin{bmatrix}0&0&0&0&\frac{kd_2-k_1d_1}{m_p}&0\\0&0&0&0&-\frac{kd_2^2+k_1d_1^2}{m_p}&0\\0&0&0&0&\frac{k_1d_1}{m_{pb}}&0\\0&0&0&0&0&0\\0&0&0&0&0&0\\0&0&0&0&0&0\end{bmatrix},\quad C_1=C_2=C_3=\begin{bmatrix}0&0&0&1&0&0\\0&0&0&0&1&0\\0&0&0&0&0&1\end{bmatrix},$$

$$D'_1=\begin{bmatrix}0&0\\0&0\\\frac{c_3}{m_{pb}}&\frac{k_3}{m_{pb}}\\0&1\\0&1\\0&1\end{bmatrix},\quad D'_2=\begin{bmatrix}0&0\\0&0\\\frac{c_4}{m_{tb}}&\frac{k_4}{m_{tb}}\\0&1\\0&1\\0&1\end{bmatrix},\quad D'_3=\begin{bmatrix}0&0\\0&0\\\frac{c_3}{m_{pb}}&\frac{k_3}{m_{pb}}\\0&1\\0&1\\0&1\end{bmatrix}.$$

$x(t) \in R^{18}$ is the state defined for the center of gravity of the cars and bogies, in which $x_{1,\cdots,6}(t) = [\dot{y}_1(t),\ \dot{\theta}_1(t),\ \dot{y}_4(t),\ y_1(t),\ \theta_1(t),\ y_4(t)]$, $x_{7,\cdots,12}(t) = [\dot{y}_2(t),\ \dot{\theta}_2(t),\ \dot{y}_5(t),\ y_2(t),\ \theta_2(t),\ y_5(t)]$ and $x_{13,\cdots,18}(t) = [\dot{y}_3(t),\ \dot{\theta}_3(t),\ \dot{y}_6(t),\ y_3(t),\ \theta_3(t),\ y_6(t)]$.
$x_1 = \dot{y}_1$ the vertical velocity of car 1,
$x_2 = \dot{\theta}_1$ the pitch angle velocity of car 1,
$x_3 = \dot{y}_4$ the vertical velocity of bogie 1,
$x_4 = y_1$ the vertical displacement of car 1,
$x_5 = \theta_1$ the pitch angle of car 1,
$x_6 = y_4$ the vertical displacement of bogie 1,
$x_7 = \dot{y}_2$ the vertical velocity of car 2,
$x_8 = \dot{\theta}_2$ the pitch angle velocity of car 2,
$x_9 = \dot{y}_5$ the vertical velocity of bogie 2,
$x_{10} = y_2$ the vertical displacement of car 2,
$x_{11} = \theta_2$ the pitch angle of car 2,
$x_{12} = y_5$ the vertical displacement of bogie 2,
$x_{13} = \dot{y}_3$ the vertical velocity of car 3,
$x_{14} = \dot{\theta}_3$ the pitch angle velocity of car 3,
$x_{15} = \dot{y}_6$ the vertical velocity of bogie 3,
$x_{16} = y_3$ the vertical displacemen of car 3,
$x_{17} = \theta_3$ the pitch angle of car 3,
$x_{18} = y_6$ the vertical displacement of bogie 3.
$g(x,t) \in R^{18} = [0,\ 0,\ 0,\ 0,\ \sin x_5(t),\ 0,\ 0,\ 0,\ 0,\ 0,\ \sin x_{11}(t),\ 0,\ 0,\ 0,\ 0,\ 0,\ \sin x_{17}(t),\ 0]^T$. $z(t) \in R^9 = [x_4(t),\ x_5(t),\ x_6(t),\ x_{10}(t),\ x_{11}(t),\ x_{12}(t),\ x_{16}(t),\ x_{17}(t),\ x_{18}(t)]^T$ is the system output vector available from sensors. $d(t) \in R^6 = [y_7(t),\ \dot{y}_7(t),\ y_8(t),\ \dot{y}_8(t),\ y_9(t),\ \dot{y}_9(t)]$ is the unknown disturbance caused by the track irregularity. $f(t) \in R^p$ with $p \leq 9$ represents the sensors fault with the distribution matrix F_s representing the fault occurring locations. $\delta'(t) \in R^{18}$ and $\eta(t) \in R^9$ are process and measurement noise described as independent zero mean white noise sequences with covariance matrices $Q'_{18\times18}(t)$ and $R_{9\times9}(t)$ respectively, where $Q'(t) = diag\{(q')_1^2(t), (q')_2^2(t), \ldots, (q')_{18}^2(t)\}$ and $R(t) = diag\{r_1^2(t), r_2^2(t), \ldots, r_9^2(t)\}$.

Remark 1: Compared with the model proposed in [2], [3], [26], the nonlinear term $g(x,t)$ exists in the suspension system (1)-(2). The movements of the suspension mounting and the articulation (end) positions of the rail vehicles are depicted as $y_{10} = y_1 - d_1\sin(\theta_1)$, $y_{12} = y_1 - d_2\sin(\theta_1)$, $y_{13} = y_2 - d_3\sin(\theta_2)$, $y_{24} = y_2 - d_3\sin(\theta_2)$, $y_{23} = y_3 - d_2\sin(\theta_3)$, $y_{11} = y_3 - d_1\sin(\theta_3)$, which lead to the nonlinear system (1)-(2). The nonlinear system (1)-(2) can be approximated by a linear form in [3], and the proposed method in this paper can be applied to the linear model. □

B. Discrete-time model

Consider discrete-time controllers used in the suspension systems, which is implemented via computer. For the future semi-physical simulation, considering the requirements from the rail vehicle company, the discrete-time model based fault scheme is discussed in this paper. In connected with this, the plant is discretized, firstly.

Set the sampling time T. Using the Euler discretization method, the continuous state-space model (1)-(2) can be discretized in the discrete state-space as:

$$x(k+1) = Ax(k) + Bg(x,k) + Dd(k) + \delta(k) \quad (3)$$

$$z(k) = Cx(k) + F_s f(k) + \eta(k) \quad (4)$$

where $A = I + TA'$, $B = TB'$, $D = TD'$, $\delta(k) = T\delta'(k)$ with covariance matrices $Q(k) = diag\{q_1^2(k), q_2^2(k), \ldots, q_{18}^2(k)\}$ and the other matrices are the same as those of system (1)-(2).

Remark 2: There are a number of sensors mounted on the rail vehicle suspension systems, such as angular velocity sensors, displacement sensors, acceleration sensors, and so on. These sensors may have faults, such as drift, bias, and freezing etc., which may be constant, time-varying and random. Here, the general fault form is considered, which may have any fault mode. □

Remark 3: For suspension systems (1)-(2) or (3)-(4), the modelling uncertainties are described as the unknown disturbance $d(t)$ and stochastic noises ($\delta(k)$ and $\eta(k)$), which are generated by the track irregularity and some electrical components. The zero mean white noise is the popular noise

description for research. For the other noises, if the probability density function is known, the method in the following section can be applied as well. □

C. Problem statement

In this paper, the objective is to develop a sensor fault detection scheme with some detection rates for the suspension system described by (3)-(4), in which track irregularity is modeled as unknown external disturbance, and processing and sensor noise are modeled as stochastic zero mean white noise. The main task in this paper is to find a effective residual generation method and the thresholds chosen way under certain disturbances with stochastic signal. To solve such a problem, the following technical issues are summarized and need to be solved:

1) In fault-free case, design a fault detection observer to estimate the state $x(k)$ and disturbance $d(k)$ to guarantee that the observer error $e(k) = [\hat{x}^T(k) - x^T(k) \quad \hat{d}^T(k) - d^T(k)]^T$ dynamics is stochastically stable, i.e., $||e(k)||^E \leqslant \chi$, where $\hat{x}(k)$ and $\hat{d}(k)$ are the estimates of the system state $x(k)$ and disturbance $d(k)$, respectively. $||e(k)||^E = E\left\{e^T(k)e(k)\right\}^{1/2}$ and $\chi > 0$ is a scalar.
2) In the faulty case, use the designed observer to generate the fault detection residual $r(k)$ and calculate the residual to obtain the statics characters for fault detection scheme design, in which the fault information $f(k)$ and the inevitable stochastic noises $\delta(k)$ and $\eta(k)$ must be contained in the residual.
3) Based on the statics characters of residual and considering the detection rates (false alarm and missing alarm rate), analyze the relations among the residual, thresholds and noises to obtain the condition that can guarantee the fault detection scheme effectively.

Under the proposed fault detection framework, the observer can estimate the system state and disturbance under the fault-free case, which also can be used as an estimation observer for controller design. For fault detection, the detection rates, such as false alarm and missing alarm rate, will be discussed and used to determine the thresholds for fault detection.

III. Fault detection observer

Fault detection scheme includes two steps: generating residual and making decision. The purpose of residual generation is to generate a fault indicating residual signal, using available information from the monitored system to extract fault symptoms from the system. There are a lot of methods to generate the residual, in which observer-based method has been widely used. In this section, the fault detection observer is designed to obtain the residual, and then analysis of the residual will be given to help making decision design.

A. Fault detection observer design

According to the form of system (3)-(4), it should be noted that there exists disturbance, which makes it difficult to generate residual to eliminate the effect from the disturbance. To solve this problem, a new vector $\omega(k) = [x^T(k) \quad d^T(k)]^T$ is introduced. Then, the system (3)-(4) can be rewritten as:

$$E\omega(k+1) = \bar{A}\omega(k) + Bg(x,k) + \delta(k) \tag{5}$$
$$z(k) = \bar{C}\omega(k) + F_s f(k) + \eta(k) \tag{6}$$

where $E = [I_{18} \quad 0_{18\times 6}]$, $\bar{A} = [A \quad D]$ and $\bar{C} = [C \quad 0_{9\times 6}]$.

It is obvious to see that system (3)-(4) has been transformed into a singular system (5)-(6) with stochastic noises. The objective now is to design a fault detection observer and residual generator for the singular system (5)-(6). This section focuses on the fault detection observer design. Firstly, construct the following dynamic system:

$$\xi(k+1) = Y\xi(k) + Gz(k) + XBg(\hat{x},u,k) \tag{7}$$
$$\hat{\omega}(k) = \xi(k) + Mz(k) \tag{8}$$

where $\xi(k) \in R^{18+6}$ is the state, $\hat{\omega}(k) = [\hat{x}^T(k) \quad \hat{d}^T(k)]^T \in R^{18+6}$ is expected to be an estimate of $\omega(k)$. The matrices Y, X, G and M are design parameter matrices, which will be determined later.

Denote the observer error $e(k) = \hat{\omega}(k) - \omega(k)$. Then from (6) and (8), the error $e(k)$ can be expressed as

$$\begin{aligned} e(k) &= \xi(k) + Mz(k) - \omega(k) \\ &= \xi(k) + (M\bar{C} - I)\omega(k) + M\eta(k) + MF_s f(k) \end{aligned} \tag{9}$$

The purpose of the observer (7)-(8) is to make the error $e(k)$ convergent to zero or bounded to a satisfied domain in the fault-free case ($f(k) = 0$) for Eq. (9).

B. Observer performance

For the fault-free case, $f(k) = 0$, it follows from Eq. (9) that the error dynamical system can be described by

$$e(k+1) = \xi(k+1) + (M\bar{C} - I)\omega(k+1) + M\eta(k+1)$$

Define $XE + M\bar{C} - I = 0$, using Eq. (5)

$$\begin{aligned} & e(k+1) \\ &= Y\xi(k) + Gz(k) + XBg(\hat{x},k) + M\eta(k+1) \\ &\quad -X\left[\bar{A}\omega(k) + Bg(x,k) + \delta(k)\right] \\ &= Ye(k) + (YXE + G\bar{C} - X\bar{A})\omega(k) \\ &\quad +XB[g(\hat{x},k) - g(x,k)] + (G - YM)\eta(k) \\ &\quad -X\delta(k) + M\eta(k+1) \end{aligned} \tag{10}$$

If the following matrix equations hold,

$$YXE + G\bar{C} - X\bar{A} = 0$$
$$XB = 0$$

then, the error dynamical equation (10) yields

$$\begin{aligned} & e(k+1) \\ &= Ye(k) + (G - YM)\eta(k) - X\delta(k) + M\eta(k+1) \end{aligned} \tag{11}$$

Further, consider the following Lyapunov function:

$$V(k) = e^T(k)Pe(k) \tag{12}$$

where $P = P^T > 0$. The corresponding Lyapunov difference along the trajectories $e(k)$ of the error system (11) is given by:

$$\begin{aligned}
&\Delta V(k)\\
&= E\{V(k+1)\} - V(k)\\
&= E\{[e^T(k)Y^T + \eta^T(k)(G-YM)^T - \delta^T(k)X^T\\
&\quad +\eta^T(k+1)M^T]P[Ye(k) + (G-YM)\eta(k)\\
&\quad -X\delta(k) + M\eta(k+1)]\} - e^T(k)Pe(k) \qquad (13)
\end{aligned}$$

According to the distribution of $\eta(k)$ and $\delta(k)$, it follows that

$$\begin{aligned}
&\Delta V(k)\\
&= E\left\{e^T(k)Y^TPYe(k) + \delta^T(k)X^TPX\delta(k)\right.\\
&\quad +\eta^T(k+1)M^TPM\eta(k+1)\\
&\quad \left.+\eta^T(k)(G-YM)^TP(G-YM)\eta(k)\right\}\\
&\quad -e^T(k)Pe(k) \qquad (14)
\end{aligned}$$

Let $P^a = X^TPX$, $P^b = M^TPM$, $P^c = (G-NM)^TP(G-NM)$ and P^i_{mn} are the elements of the matrix P^i in the m row and n column, with $i = a, b, c$. From the characters of the stochastic noises,

$$\begin{aligned}
&\Delta V(k)\\
&= e^T(k)Y^TPYe(k) - e^T(k)Pe(k) + \sum_{i=1}^{n} P^a_{ii}q_i^2(k)\\
&\quad + \sum_{j=1}^{r} P^b_{jj}r_j^2(k+1) + \sum_{j=1}^{r} P^c_{jj}r_j^2(k) \qquad (15)
\end{aligned}$$

Denote $-\Gamma = Y^TPY - P$ and $\Omega = \sum_{i=1}^{n} P^a_{ii}q_i^2(k) + \sum_{j=1}^{r} P^b_{jj}r_j^2(k+1) + \sum_{j=1}^{r} P^c_{jj}r_j^2(k)$. It is straight forward to see that Ω is a positive constant. Further, when $\Gamma = \Gamma^T > 0$, we obtain

$$\Delta V(k) = -e^T(k)\Gamma e(k) + \Omega \le -\lambda_{min}(\Gamma)\|e(k)\|^2 + \Omega \quad (16)$$

The uniformly ultimately boundness of the estimation error is guaranteed with the proposed observer, which is summarized in the following theorem.

Theorem 1*: Consider the stochastic singular system (5) - (6) and the observer (7) - (8). Under the fault free case, the state estimation error $e(k)$ given in Eq. (9) is uniformly ultimately bounded if there exists a matrix $P = P^T > 0$ such that*

$$YXE + G\bar{C} - X\bar{A} = 0, \qquad (17)$$
$$XB = 0, \qquad (18)$$
$$XE + M\bar{C} - I = 0, \qquad (19)$$
$$Y^TPY - P < 0. \qquad (20)$$

Based on Theorem 1, we summarize the observer design algorithm as follows.

1. From $XB = 0$, obtain matrix X.
2. Use $XE + M\bar{C} - I = 0$, obtain matrix $M = (I - XE)\bar{C}^+$, where $\bar{C}^+ = (\bar{C}^T\bar{C})^{-1}\bar{C}^T$ is the generalized inverse of $\bar{C}$.
3. Obtain matrix Y, using $Y^TPY - P < 0$.
4. Obtain matrix $G = (X\bar{A} - YXE)\bar{C}^+$, from $YXE + G\bar{C} - X\bar{A} = 0$. □

In the observer design, the disturbances are augmented as a subset of states, thus, the disturbances and system states are estimated, simultaneously. Using the parameters of the suspension system given in [1], [3] and the rail vehicle company, which are shown in Table I, the designed matrices of observer can be obtained. The existences of the solutions to Eq. (17)-(20) will be discussed in the next section.

TABLE I: Vehicle parameters.

Symbol	Description	Unit	Value
m_p	Power-carbody mass	kg	10 820
I_p	Power-carbody pitch inertia	kgm^2	71 000
m_t	Trailer-carbody mass	kg	4470
I_t	Trailer-carbody pitch inertia	kgm^2	6000
m_{pb}	Power-bogie mass	kg	2940
m_{tb}	Trailer-bogie mass	kg	1150
d_1	Distance between c.g. and suspension positions of the power carbody	m	2.825
d_2	Distance between c.g. and rear positions of the power carbody	m	6
d_3	Distance between c.g. and end positions of the trailer carbody	m	1.9625
k_1	Spring constant of secondary suspension of the power carbody	N/m	560 000
c_1	Damping constant of secondary suspension of the power carbody	$N.s/m$	29 584
k_2	Spring constant of secondary suspension of the trailer carbody	N/m	1 092 000
c_2	Damping constant of secondary suspension of the trailer carbody	$N.s/m$	50 205
k_3	Spring constant of secondary suspension of the power bogie	N/m	2 400 000
c_3	Damping constant of secondary suspension of the power bogie	$N.s/m$	11 883
k_4	Spring constant of secondary suspension of the trailer bogie	N/m	3 864 000
c_4	Damping constant of secondary suspension of the trailer bogie	$N.s/m$	176 673
k	Spring constant of articulation	N/m	163 000

C. Design condition analysis

The observer has been designed in the last subsection. It is obvious that the design of observer (7)-(8) for system (5)-(6) is reduced to find the matrices Y, X, G and M such that all the conditions in Theorem 1 are satisfied. To analyze the existence of solutions of observer matrix, let us define

$$A_u = \begin{bmatrix} \bar{A} \\ 0_{6\times(18+6)} \end{bmatrix} \text{ and } \bar{A} = EA_u \qquad (21)$$

$$B_u = \begin{bmatrix} B \\ 0_{6\times 18} \end{bmatrix} \text{ and } B = EB_u \qquad (22)$$

Substituting (19) and (21) into (17)

$$Y = A_u - [M \quad T]\Theta \qquad (23)$$

where $T = G - YM$ and $\Theta = \begin{bmatrix} \bar{C}A_u \\ \bar{C} \end{bmatrix}$.

Let $E_1 = I - Y^+Y$, where $Y^+ = (Y^TY)^{-1}Y^T$ is the generalized inverse of Y. Post-multiply (23) with E_1 gives

$$A_uE_1 = [M \quad T]\Theta E_1 \qquad (24)$$

Using the definition as described in (19), (18) can be written as

$$M\bar{C}B_u = B_u \tag{25}$$

Then, Equations (24) and (25) can be augmented as follows

$$[M \quad T]\Omega = \Psi \tag{26}$$

where

$$\Omega = \begin{bmatrix} \bar{C}A_uE_1 & \bar{C}B_u \\ \bar{C}E_1 & 0 \end{bmatrix}, \quad \Psi = [A_uE_1 \quad B_u]$$

Until now, the solution problem has been transformed to solve the equation (26) for M and I. The following lemma provides the sufficient and necessary condition for the existence of the solution of (26).

***Lemma 1**: There exists solution to (26) for M and I if and only if*

$$rank \begin{bmatrix} \bar{C}A_u & \bar{C}B_u \\ \bar{C} & 0 \\ A_u & B_u \end{bmatrix} = rank \begin{bmatrix} \bar{C}A_u & \bar{C}B_u \\ \bar{C} & 0 \end{bmatrix}. \tag{27}$$

Proof: Based on the general solution of linear matrix equations, there are solutions to equation (26) if and only if

$$rank \begin{bmatrix} \Omega \\ \Psi \end{bmatrix} = rank(\Omega) \tag{28}$$

The left-hand side of (27) can be expressed as

$$\begin{aligned} &rank \begin{bmatrix} \bar{C}A_u & \bar{C}B_u \\ \bar{C} & 0 \\ A_u & B_u \end{bmatrix} \\ &= rank \left\{ \begin{bmatrix} \bar{C}A_u & \bar{C}B_u \\ \bar{C} & 0 \\ A_u & B_u \end{bmatrix} \begin{bmatrix} E_1 & 0 \\ 0 & I \end{bmatrix} \right\} \\ &= rank \begin{bmatrix} \Omega \\ \Psi \end{bmatrix} \end{aligned} \tag{29}$$

Similarly, the right-hand side of (27) can be expressed as

$$\begin{aligned} &rank \begin{bmatrix} \bar{C}A_u & \bar{C}B_u \\ \bar{C} & 0 \end{bmatrix} \\ &= rank \left\{ \begin{bmatrix} \bar{C}A_u & \bar{C}B_u \\ \bar{C} & 0 \end{bmatrix} \begin{bmatrix} E_1 & 0 \\ 0 & I \end{bmatrix} \right\} \\ &= rank(\Omega) \end{aligned} \tag{30}$$

So, it can be shown that (27) is equivalent to (29) and (30), which is equivalent to the condition in (28). This completes the proof of Lemma 1. ∇

From Lemma 1, a general solution to Eq. (27) exists if Eq. (28) holds.

Remark 4: The idea of the fault detection observer design is from the unknown input observer, which is utilized for fault detection since 1990's and is often used to deal with robust fault detection problems [6]. Until now, there exist a lot of results about the unknown input observer based fault detection, see [6], [7], [8] and [9]. Compared with the other observers, the proposed fault detection observer in this paper can handle the disturbance $d(k)$ and help to obtain the estimation error expression, which is the key procedure to generate the fault detection residual and to decide the thresholds with certain performances (false alarm and missing alarm). □

IV. Fault detection decision scheme

In order to accomplish the fault detection task, a fault indication signal, i.e. residual, should be sensitive to the sensor faults, but at the same time, insensitive to the noises. Next, a fault detection scheme based on the proposed observer is provided.

A. Fault detection residual

To detect the fault, the residual should be generated. The residual generator based on the observer design technique with the residual vector is given by

$$r(k) = S_1\xi(k) + S_2z(k) \tag{31}$$

where $r(k) \in R$, $S_1 \in R^{1\times(18+6)}$ and $S_2 \in R^{1\times9}$. The residual is used to detect the influence of the faults on the system. In the non-faulty case, the observer error is independent of the stochastic noises.

Substituting (6) and (7) into (31), residual for faulty case yields

$$\begin{aligned} r_f(k) = {} & S_1e(k) + (S_2\bar{C} + S_1XE)\omega(k) \\ & + (S_2 - S_1M)F_sf(k) + (S_2 - S_1M)\eta(k) \end{aligned} \tag{32}$$

From Eq. (32), the disturbance effect has been explicitly decoupled from the error dynamics and the residual expression. The faults can be detected, if the residual expression is independent of the state vector, which requires that

$$S_2\bar{C} + S_1XE = 0 \tag{33}$$

and

$$S_2 - S_1M \neq 0 \tag{34}$$

Choose appropriate matrices S_1 and S_2 satisfying both conditions (33) and (34). Then the noise term appears in the residual, which can be presented as

$$\begin{aligned} r_f(k) = {} & S_1e(k) + (S_2 - S_1M)F_sf(k) \\ & + (S_2 - S_1M)\eta(k) \end{aligned} \tag{35}$$

When a fault occurs in the plant, the state estimation error (or residual vector) changes, and hopefully so does its mean vector. The situation in which the fault effect is reflected on the residual mean, as generic, is focused in the subsequent analysis.

For no fault case $f(k) = 0$, it can be obtained from (11), that

$$\begin{aligned} e(k) = {} & Y^ke(0) + \sum_{n=0}^{k-1} Y^{k-n-1}(G - YM)\eta(n) \\ & + \sum_{n=1}^{k} Y^{k-n}M\eta(n) - \sum_{n=0}^{k-1} Y^{k-n-1}X\delta(n) \end{aligned} \tag{36}$$

Due to the Gaussian process noises $\eta(k)$ and $\delta(k)$, $e(k)$ is also a Gaussian process, whose mean and variance can be

calculated as follows:

$$
\begin{aligned}
&E\{e(k)\} = Y^k e(0) \qquad (37)\\
&Var\{e(k)\}\\
=&E\{[e(k)-E\{e(k)\}]\cdot[e(k)-E\{e(k)\}]^T\}\\
=&\sum_{n=1}^{k-1}[Y^{k-n-1}(G-YM)+Y^{k-n}M]R(n)\\
&\times[(G-YM)^T(Y^{k-n-1})^T+M^T(Y^{k-n})^T]\\
&+Y^{k-1}(G-YM)R(0)(G-YM)^T(Y^{k-1})^T\\
&+MR(k)M^T+\sum_{n=0}^{k-1}Y^{k-n-1}XQ(n)X^T(Y^{k-n-1})^T\\
\triangleq&T_e(k) \qquad (38)
\end{aligned}
$$

Therefore, $e(k)\sim\mathcal{N}(Y^k e(0), T_e(k))$. Further, the residual for faulty-free case is represented as

$$r_h(k) = S_1 e(k) + (S_2 - S_1 M)\eta(k) \qquad (39)$$

Define $T_r(k) \triangleq S_1 T_e(k) S_1^T + (S_2 - S_1 M)R(k)(S_2 - S_1 M)^T - S_1 Y^k e(0) e^T(0)(Y^k)^T S_1^T$. Using Eq. (39), the mean and variance of the residual can be calculated $r_h(k) \sim \mathcal{N}(S_1 Y^k e(0), T_r(k))$.

On the other hand, for the faulty case, $f(k)\neq 0$, the residual is presented as

$$
\begin{aligned}
r_f(k) =& S_1 e(k) + (S_2 - S_1 M)\eta(k)\\
&+(S_2 - S_1 M)F_s f(k) \qquad (40)
\end{aligned}
$$

It is obvious that the faulty residual $r_f(k)$ is also the Gaussian process, whose mean and variance can be calculated $r_f(k)\sim\mathcal{N}(S_1 Y^k e(0)+(S_2-S_1M)F_s f(k), T_r(k))$.

B. Probabilistic residual evaluation

According to residual (39) and (40), the change of the mean implies that the faults just appeared. So, the following hypothesis test can be presented:

$$H_0 : E\{r(k)\} = S_1 Y^k e(0), \quad H_1 : E\{r(k)\} \neq S_1 Y^k e(0)$$

Here, $r(k)$ itself is chosen as the mean estimator, which is the Gaussian process. Then the acceptance region of the test $B(k)$ can be assumed to satisfy

$$P(r(k)\in B(k)|H_0) = 1-\lambda \qquad (41)$$

where λ is positive with a small value previously chosen which constitutes the test size.

A natural measure of the distance from $r(k)$ to $E\{r(k)|H_0\}$ is the Mahalanobis distance defined as

$$d_M(r(k), E\{r(k)|H_0\}) = \frac{|r(k)-E\{r(k)|H_0\}|}{\sqrt{Var_{r(k)|H_0}}} \qquad (42)$$

The test acceptance region will be the circle defined by

$$B(k) = \{\xi\in\Re : d_M(\xi, E\{r(k)|H_0\}) \leqslant k_\lambda\}$$

where the operator $d_M(\cdot,\cdot)$ is given in (42) and the radius k_λ is to be determined from the condition (41). Specifically, for a Gaussian mean estimator, $k_\lambda = h_{\lambda/2}$.

Therefore, the test acceptance region $B(k)$ can take the form of an interval as

$$
\begin{aligned}
B(k) =& [l(k), u(k)]\\
=&\Big[S_1 Y^k e(0) - h_{\lambda/2}\sqrt{Cov\{r_h(k)/H_0\}}\,,\\
&S_1 Y^k e(0) + h_{\lambda/2}\sqrt{Cov\{r_h(k)/H_0\}}\Big] \qquad (43)
\end{aligned}
$$

where $Cov\{r_h(k)|H_0\} = T_r(k)$ and $h_{\lambda/2}$ means that the standard normal distributed variable has the probability of $\lambda/2$ to fall into $[h_{\lambda/2}, +\infty)$.

According to the above results, the following fault detection decision can be formed: if $r(k)\notin B(k)$, a fault has likely occurred in plant, where the instant time when the fault is detected can be defined by the random variable $T_d = \inf\{k > T_0 : r(k)\notin B(k)\}$, T_0 is the unknown instant when the fault occurs. As a quality measure index of such tests, the false alarm rate is given by:

$$P(D_{test}(k) = H_1|H_0) = 1 - P(r(k)\in B(k)|H_0) = \lambda \qquad (44)$$

where $D_{test}(k)$ is the test decision at instant k.

Further, when the fault occurs (consequently $k > T_0$), there also exists a confidence region $A(k)\subset R$, in which $(1-\upsilon)$ of the mean estimator realizations remain at instant k. In particular, that region will be symmetric with respect to $E\{r(k)|H_1\}$ such that

$$P(r(k)\in A(k)|H_1) = 1-\upsilon, \qquad k > T_0 \qquad (45)$$

The same as the approach of computing the acceptance region $B(k)$, the confidence region $A(k)$ can be obtained by:

$$
\begin{aligned}
&A(k)\\
=&[a(k), b(k)]\\
=&\Big[S_1 Y^k e(0) + (S_2 - S_1 M)F_s f(k) - h_{\upsilon/2}\sqrt{Cov\{r_f(k)/H_1\}}\,,\\
&S_1 Y^k e(0) + (S_2 - S_1 M)F_s f(k) + h_{\upsilon/2}\sqrt{Cov\{r_f(k)/H_1\}}\Big]
\end{aligned}
$$

Therefore, if $\hat{T}_d < +\infty$, then the fault is detectable with $\hat{T}_d = \inf\{k\geq T_0 : A(k)\cap B(k) = \emptyset\}$.

C. Fault detectability analysis

Based on the analysis above, necessary fault detectability conditions can be presented. Intuitively, a fault is detectable if there exists time $T_d < +\infty$, in which the mean estimator realization crosses the bounds of the test acceptance region, which occurs for most realizations. This idea is formalized in the probabilistic environment, concluding in a probabilistic definition of fault detectability.

Theorem 2*: For a fault $f(k)$ with its ith element satisfying $|f_i(k)|\geqslant\varepsilon$, $\forall k > T_0$, $i = 1,\ldots,p$ and a fixed value $\upsilon\in(0,1)$, a sufficient and necessary condition to assure the existence of a finite value $\hat{T}_d\geqslant T_0$ such that the fault $f(k)$ can be detectable by the FD scheme associated with residual $r(k)$, is*

$$
\begin{aligned}
\varepsilon > \varepsilon_0 = \frac{1}{\|(S_2 - S_1 M)F_s\|}\Big(&h_{\lambda/2}\sqrt{Cov\{r_h(k)/H_0\}}\\
&+h_{\upsilon/2}\sqrt{Cov\{r_f(k)/H_1\}}\Big) \qquad (46)
\end{aligned}
$$

Proof: Using the residual $r(k)$ in Eq. (40) and taking into account the linearity of the mean operator, it follows that

$$E\{r_f(k)|H_1\} = E\{r_h(k)|H_0\} + (S_2 - S_1M)F_s f(k) \quad (47)$$

Denote $\Phi(f(k)) = (S_2 - S_1M)F_s f(k)$.

Sufficiency: i) When $\Phi(f(k)) > 0$, it is related to the situation $f(k) \geqslant \varepsilon$, $\forall k > T_0$. Condition (46) is satisfied, which implies $\exists\, k > T_0$ such that

$$\begin{aligned}&\Phi(f(k))\\ &> \left(h_{\lambda/2}\sqrt{Cov\{r_h(k)/H_0\}} + h_{\upsilon/2}\sqrt{Cov\{r_f(k)/H_1\}}\right)\end{aligned}$$

Therefore

$$\begin{aligned}&\{k \geq T_0 : a(k) \geq u(k)\}\\ &= \Big\{k \geq T_0 : E\{r_f(k)|H_1\} - h_{\upsilon/2}\sqrt{Cov\{r_f(k)/H_1\}}\\ &\qquad \geq E\{r_h(k)|H_0\} + h_{\lambda/2}\sqrt{Cov\{r_h(k)/H_0\}}\Big\}\\ &= \{k \geq T_0 : E\{r_f(k)|H_1\} - E\{r_h(k)|H_0\}\\ &\quad \geq h_{\lambda/2}\sqrt{Cov\{r_h(k)/H_0\}} + h_{\upsilon/2}\sqrt{Cov\{r_f(k)/H_1\}}\Big\}\\ &\supseteq \Big\{k \geq T_0 : \Phi(f(k)) > h_{\lambda/2}\sqrt{Cov\{r_h(k)/H_0\}}\\ &\qquad + h_{\upsilon/2}\sqrt{Cov\{r_f(k)/H_1\}}\Big\}\\ &\supseteq [k^*, +\infty) \neq \emptyset \qquad (48)\end{aligned}$$

So

$$\exists\, \hat{T}_d = \inf\{k \geq T_0 : a(k) \geq u(k)\} \leq k^* \leq +\infty$$

ii) When $\Phi(f(k)) \leqslant 0$, it means that $f(k) \leqslant -\varepsilon$, $\forall k > T_0$. The fact that condition (46) is satisfied, implies that $\exists\, k > T_0$ fulfills that

$$\begin{aligned}&\Phi(f(k))\\ &< -\left(h_{\lambda/2}\sqrt{Cov\{r_h(k)/H_0\}} + h_{\upsilon/2}\sqrt{Cov\{r_f(k)/H_1\}}\right)\end{aligned}$$

Therefore

$$\begin{aligned}&\{k \geq T_0 : b(k) \leq l(k)\}\\ &= \Big\{k \geq T_0 : E\{r_f(k)|H_1\} + h_{\upsilon/2}\sqrt{Cov\{r_f(k)/H_1\}}.\\ &\qquad \leq E\{r_h(k)|H_0\} - h_{\lambda/2}\sqrt{Cov\{r_h(k)/H_0\}}\Big\}\\ &= \{k \geq T_0 : E\{r_f(k)|H_1\} - E\{r_h(k)|H_0\} \leq\\ &\quad -\left(h_{\lambda/2}\sqrt{Cov\{r_h(k)/H_0\}} + h_{\upsilon/2}\sqrt{Cov\{r_f(k)/H_1\}}\right)\Big\}\\ &\supseteq \Big\{k \geq T_0 : \Phi(f(k)) < -\Big(h_{\lambda/2}\sqrt{Cov\{r_h(k)/H_0\}}\\ &\qquad + h_{\upsilon/2}\sqrt{Cov\{r_f(k)/H_1\}}\Big)\Big\}\\ &\supseteq [k^*, +\infty) \neq \emptyset\end{aligned}$$

so

$$\exists\, \hat{T}_d = \inf\{k \geq T_0 : b(k) \leq l(k)\} \leq k^* \leq +\infty$$

Necessity: If condition (46) is not satisfied, then, when $\Phi(f(k)) > 0$, there will be the situation

$$\begin{aligned}0 < \Phi(f(k)) < \Big(&h_{\lambda/2}\sqrt{Cov\{r_h(k)/H_0\}}\\ &+ h_{\upsilon/2}\sqrt{Cov\{r_f(k)/H_1\}}\Big)\end{aligned}$$

Therefore

$$\begin{aligned}&\{k \geq T_0 : a(k) < u(k)\}\\ &= \{k \geq T_0 : E\{r_f(k)|H_1\} - E\{r_h(k)|H_0\}\\ &\quad < h_{\lambda/2}\sqrt{Cov\{r_h(k)/H_0\}} + h_{\upsilon/2}\sqrt{Cov\{r_f(k)/H_1\}}\Big\}\\ &\supseteq \Big\{k \geq T_0 : \Phi(f(k)) < \Big(h_{\lambda/2}\sqrt{Cov\{r_h(k)/H_0\}}\\ &\qquad + h_{\upsilon/2}\sqrt{Cov\{r_f(k)/H_1\}}\Big)\Big\}\end{aligned}$$

The inequality $a(k) < u(k)$ implies that there will be intersection between $B(k)$ and $A(k)$, and the detection decision may provide a wrong alarm, which means the faults may not be detected. Actually, the derivation above is also valid in the situation $\Phi(f(k)) < 0$. So, it is obtained that: If the faults would be detected, it should satisfy condition (46). From above, it follows that the fault $f(k)$ is detectable, when the conditions of Theorem 2 hold. ∇

Remark 5: The above fault detection design and performance analysis are dependent on the evaluation function chosen as the residual directly. In fact, there are varieties of the evaluation function generation methods, such as $r^T(k)r(k)$, $\sum_{k=0}^{n} r(k)$ with n steps, $|r(k)|$ and so on. With the different evaluation functions, the stochastic character parameters (mean and variance) can also be calculated. Therefore, the proposed fault detection method and performance analysis can be easily extended to the other evaluation function cases. □

Remark 6: The faults considered in this paper only affect the mean of the residual, instead of the variance. So Eq. (46) can be used to obtain the necessary condition for fault when the fault information is not available completely. For random faults, the means and variances of faults should be known. Otherwise Theorem 2 cannot be used. □

D. Discussion

Usually, the detection power of the test θ or its complement, the missed detection rate, $1 - \theta$ is considered. The missed detection rate is defined as

$$1 - \theta = 1 - P(D_{test}(k) = H_1|H_1) = P(r_f(k) \in B(k)|H_1)$$

In case that the fault process $f(k)$ satisfies any of the given sufficient detectability conditions associated with the residual, then, as shown in the proof of Theorem 2, $\exists\, k^* \geqslant \widehat{T}_d$ such that

$$\begin{aligned}a(k) \geq u(k), \quad \forall k^* \geq \hat{T}_d\\ \theta > P(r(k) > u(k)|H_1) \geq P(r(k) > a(k)|H_1)\\ P(r(k) > a(k)|H_1) = 1 - \frac{\upsilon}{2}, \quad \forall k^* \geq \hat{T}_d\end{aligned}$$

Therefore, the missed detection rate is

$$1-\theta<\frac{\upsilon}{2},\quad \forall k^*\geq \hat{T}_d \tag{49}$$

Remark 7: All the noises considered in this paper are the Gaussian noise, which makes the hypothesis test achievable. Note that in real systems, the Gaussian noise is one of the multiple noises. For non-Gaussian noises, if their probability density functions are available, the probability density functions of the residuals and evaluation functions can also be computed. Then, in this case, the proposed method can be used to that class of systems with non-Gaussian noises. □

V. Simulation study

To verify the effectiveness of the designed fault detection strategy, a passive suspension system for city metro is simulated in the presence of sensor faults.

A. Simulation system

The systems parameters and variables considered in the simulation are given in Table I.

Here, set the sampling time $T = 0.001\,\text{sec}$. For simulation purpose, the initial conditions are set as $x(0) = 0.01[\underbrace{1,1,\ldots,1}_{18}]^T$ and $\hat{x}(0)=0$.

The track irregular is considered as the disturbance $d(k)$. Choose $y_7(k) = y_9(k) = \sin(0.01\pi k)$, $y_8(k) = 0.1\sin(0.01\pi k)$ and $\Delta y_7(k) = \Delta y_9(k) = 0.01\pi\cos(0.01\pi k)$, $\Delta y_8(k) = 0.001\pi\cos(0.01\pi k)$. Choose the covariance matrices for noise sequences of process and measurement $Q(k) = 0.01^2 \times I_{18\times 18}$ and $R(k) = 0.01^2 \times I_{9\times 9}$, respectively.

Assume a fault occurs in the sensors of the third carbody, and the fault distribution matrix F_s is chosen as $F_s = [\ 0\quad 0\quad 0\quad 0\quad 0\quad 0\quad 1.2\quad 0.6\quad 1\ ]^T$ with the fault expressed in two cases:

$$\textit{Case}\ \ 1: f_1(k) = \begin{cases} 0 & 0<k<4(sec) \\ f_1^0 & 4(sec)\leq k \end{cases} \tag{50}$$

$$\textit{Case}\ \ 2: f_2(k) = \begin{cases} 0 & 0<k<4(sec) \\ (1-e^{-0.8(k-4)})f_2^0 & 4(sec)\leq k \end{cases} \tag{51}$$

where f_1^0 and f_2^0 are the fault amplitude parameters of the abrupt and incipient fault, respectively. The abrupt fault occuring at the sec. 4, can be considered as the sensor drift. The incipient fault could be influenced by the change of sensor temperature, which occures at the sec. 4.

B. Simulation results

Using Theorem 1, the observer matrices X, M and G can be obtained. The responses of the health system to the observer are shown in Fig. 3-6.

The responses of the health system to the observer are shown in Figs. 3-6. Then, the following faulty cases will be discussed.

Case 1 (abrupt fault f_1): Set $\lambda = \upsilon = 0.06$ as test size in Eq. (41) and (45), respectively, which means that the false alarm rate is 6%. Then, the test acceptance region $B(k)$ in Eq. (43) can be calculated as:

$$[S_1Y^ke(0) - 1.88\sqrt{Cov\{r_h(k)/H_0\}},\\ S_1Y^ke(0) + 1.88\sqrt{Cov\{r_h(k)/H_0\}}] \tag{52}$$

The condition for fault detection is given as follows:

$$f(k) > \frac{1}{\|(S_2-S_1M)F_s\|}\Big(h_{\lambda/2}\sqrt{Cov\{r_h(k)/H_0\}} \\ +h_{\upsilon/2}\sqrt{Cov\{r_f(k)/H_1\}}\Big) = 0.2961 \tag{53}$$

Let the parameters $f_1^0 = 0.2$ and 0.4. Then the fault detection simulation result given in Fig. 7.

Case 2 (incipient fault f_2): Choose $\lambda = \upsilon = 0.03$, which means that the false alarm rate is 3%. Similar to case 1, the test acceptance region $B(k)$ in Eq. (43) can be calculated as:

$$[S_1Y^ke(0) - 2.17\sqrt{Cov\{r_h(k)/H_0\}},\\ S_1Y^ke(0) + 2.17\sqrt{Cov\{r_h(k)/H_0\}}] \tag{54}$$

The sufficient condition under which the fault (assuming positive fault) can be detected is $f(k) > 0.3418$. Choose the fault parameters $f_2^0 = 0.25$ and 0.45. The fault detection simulation result is shown in Fig. 8.

C. Discussion

Explanation for Figs. 3-6. Figs. 3-6 show the state and disturbance estimation performance of the observer for the three carbodies. The states and disturbances y_3, θ_3, y_6, Δy_3, $\Delta\theta_3$, Δy_6, y_9 and Δy_9 of the second power carbody are largely the same as those of the first power carbody, whose simulation results are omitted here. Due to the noises, some displacements (sataes) of the carbody cannot converge to zero. From figs. 3-6, it can be seen that in the fault-free case, the proposed observer can track the states and disturbances with small errors, even under the noises environment, which verifies the effectiveness of the proposed observer.

Explanation for Fig. 7. (a) before $t < 4\,\text{sec}$., the residual within the thresholds indicates fault free and its values that exceed the thresholds indicate the false alarm time instants. After 4 sec., the residual is shifted due to fault. The figure indicates that there is a fault but its amplitude may be small (because the residual is both above and below the upper threshold). The residual values within the thresholds indicate the missing alarm time instants (related to υ given (49)). This subfigure indicates for this fault amplitude $0.2 < 0.2961$ (which does not satisfy the fault detection condition given in Eq. (53)), the fault cannot be effectively detected. (b) Before 4 sec., the residual is the same as that in (a), which indicates fault free with 6% false alarm. After 4 sec., the residual mostly exceeds the upper threshold, which confirms the fault occurrence. The values of residual within the thresholds also indicate the missing alarm time instants which are much less than that in (a). In this case, for the fault amplitude $0.4 > 0.2961$ (which satisfies the amplitude condition in Eq. (53)), the fault can be effectively detected.

Explanation for Fig. 8. (a) Similar to the in Figure 7, before $t < 4\,\text{sec}$., the residual within the thresholds indicates fault

free and its values that exceed the thresholds indicate the false alarm time instants. After 4 sec., the residual is shifted due to fault. The figure indicates that there is a fault but its amplitude may be small (because the residual is both above and below the upper threshold). The residual values within the thresholds indicate the missing alarm time instants (related to υ given (49)). This subfigure indicates for this fault amplitude $0.25 < 0.3418$ (which does not satisfy the fault detection condition given in Eq. (53)), the fault cannot be effectively detected. (b) Before 4 sec., the residual is the same as that in (a), which indicates fault free with 6% false alarm. Between 4 to 5 sec., the residual is also within the thresholds but ascends slowly, since fault 2 is a incipient fault. After 5 sec., the residual mostly exceeds the upper threshold, which confirms the fault occurrence. The values of residual within the thresholds also indicate the missing alarm time instants which are much less than that in (a). In this case, for the fault amplitude $0.45 > 0.3418$ (which satisfies the amplitude condition in Eq. (53)), the fault can be effectively detected.

Comparisons between Figs. 7 and 8. Figs. 7 and 8 show the fault detection residuals for two faulty cases, with the different thresholds determined by different choices of false alarm parameters. The observer states and the system outputs are used to generate the residual designed in Eq. (31). The

$$X = \begin{bmatrix}
2.5022 & -2.7365 & 1 & 0.5200 & -0.2460 & 0.0200 & 0 & 0 & -0.0100 & 1 & 0.2633 & -0.3696 & 0 & 0 & 0 & 1 & 0 & 1 \\
0 & 0 & 0 & 1.0000 & 1.2285 & 0.6227 & 0 & 0 & 2.5800 & 0 & 0.4931 & 1.8160 & 0 & 0 & 0 & 0.7619 & 1.3446 & 0 \\
0 & 0 & 0 & 0.4725 & 1.0000 & 1 & 0 & 0 & 0.8643 & 1 & -2.5316 & 0.8813 & 0 & 0 & 0 & 1.3302 & 1 & 0.2557 \\
0 & 0 & 0 & 0.2670 & 0.3750 & 1.0000 & 0 & 0 & 1 & 0 & 1.6470 & 1 & 0 & 0 & 0 & 0.7322 & 0.6433 & 0.5469 \\
-2.2658 & -5.2630 & 0 & 1 & 0.1057 & 0.2955 & -1.4621 & 1 & 0.4671 & 1 & 0.5386 & 0.0252 & 0 & 0 & 0 & 0.1781 & 0.8627 & 0.5590 \\
0 & 0 & 0 & 0.0616 & -0.7350 & 0.3664 & 0 & 0 & 1.0000 & 0 & 0.5832 & 0.1844 & 0 & 0 & 0 & 0.2880 & 0.0205 & 0 \\
0 & 0 & 0 & -0.3958 & 0.6948 & 0.5583 & 0 & 0 & 0 & 1 & 0 & 0.9335 & 0 & 0 & 0 & 1.7157 & 0.0474 & 0.6751 \\
0 & 0 & 0 & 0.8051 & 0.0610 & -0.8588 & 0 & 0 & 0.6003 & 0 & 1.0000 & 0.0915 & 0 & 0 & 0 & 0.6500 & 0.1478 & 0.7283 \\
0 & 0 & 0 & -0.9171 & 0.4334 & 0.5573 & 0 & 0 & 0.3798 & 0 & 0.0161 & 1.0000 & 0 & 0 & 0 & 0.2144 & 0.3065 & 0.6008 \\
0 & 0 & 0 & 0.4079 & -0.8605 & 0.1682 & 0 & 0 & 0.0624 & 1 & 0.1839 & 0.7170 & 0 & 0 & 0 & 0.5652 & 0 & 0.0751 \\
0 & 0 & 0 & 0.5518 & 0.6533 & -0.9728 & 0 & 0 & 0.1874 & 0 & 0.8721 & 0.6125 & 0 & 0 & 0 & 0.0381 & 0.8412 & 0.4471 \\
0 & 0 & 0 & 0.6357 & 0.1005 & 0.7985 & 0 & 0 & -0.8797 & 0 & 0.7352 & 0.0185 & 0 & 0 & 0 & 0.3202 & 0.1109 & 0.2483 \\
1.0000 & 0 & 0 & 0.7537 & 0.1048 & 0.8271 & -0.2551 & 0 & 0.3400 & 0 & 0.8467 & 0.2461 & 1.0000 & 0 & 0 & 0.7337 & 0.4068 & 1 \\
0.0000 & -1.0000 & 0 & 0.2886 & 0.3796 & 0.9460 & -0.6654 & 0 & 0.7467 & 1 & 0.3892 & 0.9053 & 0 & 1 & 0 & 0.2433 & 0 & 0.3788 \\
-2.5022 & 2.7365 & 0 & -0.9812 & 0.8610 & 0.4076 & 2.4594 & 0 & 0.3270 & 0 & 0.4030 & 0.5209 & 0 & 0 & 1.0000 & 0.3751 & 0.0536 & 0.2395 \\
0 & 0 & 0 & 0.5470 & -0.9223 & 0.3632 & 0 & 0 & 0.4590 & 0 & 0.8177 & 0.1051 & 0 & 0 & 0 & 1.0000 & 0.0610 & 0.4730 \\
0 & 0 & 0 & -0.7061 & 0.6871 & 0.1411 & 0 & 0 & 0.5953 & 0 & 0.8288 & 0.5953 & 0 & 0 & 0 & 0 & 1.0000 & 0 \\
0 & 0 & 0 & 0.1411 & 0.5121 & -0.7529 & 0 & 0 & 0.3225 & 0 & 0.7040 & 0.0843 & 0 & 0 & 0 & 0.9015 & 0 & 1.0000 \\
1 & 0 & 0 & 1 & 1 & 1 & -0.2550 & 0 & 1 & 1 & 1 & 1 & 1 & 0 & 0 & 1 & 1 & 1 \\
0 & 1 & 0 & 1 & 1 & 1 & 0.6654 & 0 & 1 & 1 & 1 & 1 & 0.9122 & 0 & 0.3652 & 1 & 1 & 1 \\
0.2364 & -7.9995 & 1 & 0.2072 & 0.2457 & 0.2870 & -1.4621 & 1 & 0.4929 & 0 & 0.1428 & 0.7811 & 0 & 0 & 0 & 0.5862 & 0.2629 & 0.1957 \\
-1.2658 & -5.2630 & 0 & 0.9716 & 0.4429 & 0.0261 & -1.7172 & 1 & 0.3879 & 0 & 0.1789 & 0.6581 & 1 & 0 & 0 & 0.4967 & 0.1816 & 0.4324 \\
1 & -1 & 0 & 0.6343 & 0.9265 & 0.5936 & -0.9205 & 0 & 0.8836 & 1 & 0.9092 & 0 & 1 & 1 & 0 & 0.3753 & 0.2138 & 0.6329 \\
-2.5022 & 1.7365 & 0 & 0.2293 & 0.6113 & 0.2313 & 1.7940 & 0 & 0.6894 & 0 & 0.0516 & 0 & 0 & 1 & 1 & 0.4265 & 0.3764 & 0.9971
\end{bmatrix}$$

$$M = \begin{bmatrix}
-0.5200 & 2.7365 & -0.0200 & -1.0000 & 0 & 0.3696 & -1.0000 & 0 & -1.0000 \\
-1.0000 & 1.0000 & -0.6227 & 0 & 0 & -1.8160 & -0.7619 & 0 & 0 \\
-0.4725 & 0 & -1.0000 & -1.0000 & 0 & -0.8813 & -1.3302 & 0 & -0.2557 \\
0.7330 & 0 & -1.0000 & 0 & 0 & -1.0000 & -0.7322 & 0 & -0.5469 \\
-1.0000 & 5.2630 & -0.2955 & -1.0000 & -1.0000 & -0.0252 & -0.1781 & 0 & -0.5590 \\
-0.0616 & 0 & 0.6336 & 0 & 0 & -0.1844 & -0.2880 & 0 & 0 \\
0.3958 & 0 & -0.5583 & -1.0000 & 0 & -0.9335 & -1.7157 & 0 & -0.6751 \\
-0.8051 & 0 & 0.8588 & 0 & 1.0000 & -0.0915 & -0.6500 & 0 & -0.7283 \\
0.9171 & 0 & -0.5573 & 0 & 0 & -1.0000 & -0.2144 & 0 & -0.6008 \\
-0.4079 & 0 & -0.1682 & 0 & 0 & -0.7170 & -0.5652 & 0 & -0.0751 \\
-0.5518 & 0 & 0.9728 & 0 & 0 & -0.6125 & -0.0381 & 0 & -0.4471 \\
-0.6357 & 0 & -0.7985 & 0 & 0 & 0.9815 & -0.3202 & 0 & -0.2483 \\
-0.7537 & 0 & -0.8271 & 0 & 0 & -0.2461 & -0.7337 & 0 & -1.0000 \\
-0.2886 & 1.0000 & -0.9460 & -1.0000 & 0 & -0.9053 & -0.2433 & 0 & -0.3788 \\
0.9812 & -2.7365 & -0.4076 & 0 & 0 & -0.5209 & -0.3751 & 0 & -0.2395 \\
-0.5470 & 0 & -0.3632 & 0 & 0 & -0.1051 & 0 & 0 & -0.4730 \\
0.7061 & 0 & -0.1411 & 0 & 0 & -0.5953 & 0 & 0 & 0 \\
-0.1411 & 0 & 0.7529 & 0 & 0 & -0.0843 & -0.9015 & 0 & 0 \\
-1.0000 & 0 & -1.0000 & -1.0000 & 0 & -1.0000 & -1.0000 & 0 & -1.0000 \\
-1.0000 & -1.0000 & -1.0000 & -1.0000 & 0 & -1.0000 & -1.0000 & 0 & -1.0000 \\
-0.2072 & 7.9995 & -0.2870 & 0 & -1.0000 & -0.7811 & -0.5862 & 0 & -0.1957 \\
-0.9716 & 5.2630 & -0.0261 & 0 & -1.0000 & -0.6581 & -0.4967 & 0 & -0.4324 \\
-0.6343 & 1.0000 & -0.5936 & -1.0000 & 0 & 0 & -0.3753 & -1.0000 & -0.6329 \\
-0.2293 & -1.7365 & -0.2313 & 0 & 0 & 0 & -0.4265 & -1.0000 & -0.9971
\end{bmatrix},$$

$$G = \begin{bmatrix}
0.8840 & -4.6523 & -0.7823 & 1.6905 & 0.0003 & -0.5852 & 1.7000 & 0 & 1.7000 \\
1.7000 & 0.0012 & 1.0586 & 2.4499 & 0.0005 & -8.0315 & 1.2952 & 0.0013 & 0 \\
0.8033 & 0.0010 & 1.7000 & 2.5207 & -0.0025 & -2.2265 & 2.2613 & 0.0010 & 0.4347 \\
0.4539 & 0.0004 & 1.7000 & 0.9496 & 0.0016 & -2.6096 & 1.2447 & 0.0006 & 0.9297 \\
1.7000 & -8.9470 & 0.5023 & 2.5007 & 1.7005 & -2.3273 & 0.3028 & 0.0009 & 0.9503 \\
0.1047 & -0.0007 & 0.6229 & 0.9496 & 0.0006 & -3.9961 & 0.4896 & 0.0000 & 0 \\
-0.6729 & 0.0007 & 0.9491 & 1.7000 & 0 & 1.5869 & 2.9167 & 0.0000 & 1.1477 \\
1.3687 & 0.0001 & -1.4600 & 0.5700 & 0.0010 & -2.4315 & 1.1050 & 0.0001 & 1.2381 \\
-1.5591 & 0.0004 & 0.9474 & 0.3606 & 0.0000 & 0.0632 & 0.3645 & 0.0003 & 1.0214 \\
0.6934 & -0.0009 & 0.2859 & 1.7593 & 0.0002 & 0.9500 & 0.9608 & 0 & 0.1277 \\
0.9381 & 0.0007 & -1.6538 & 0.1779 & 0.0009 & 0.2336 & 0.0648 & 0.0008 & 0.7601 \\
1.0807 & 0.0001 & 1.3575 & -0.8353 & 0.0007 & 3.8226 & 0.5443 & 0.0001 & 0.4221 \\
1.2052 & 0.0078 & 1.4578 & 0.4339 & 0.0008 & -1.1092 & 1.1712 & -0.0073 & 1.7518 \\
0.4578 & -1.6963 & 1.6305 & 2.5926 & 0.0004 & -1.8415 & 0.3808 & 1.6967 & 0.6662 \\
-1.3879 & 4.6245 & 0.5024 & -0.4697 & 0.0004 & 0.0771 & 0.9178 & 0.0285 & -0.5997 \\
0.9299 & -0.0009 & 0.6174 & 0.4359 & 0.0008 & -1.7994 & 1.7000 & 0.0001 & 0.8041 \\
-1.2004 & 0.0007 & 0.2399 & 0.5653 & 0.0008 & -1.5535 & 0 & 0.0010 & 0 \\
0.2399 & 0.0005 & -1.2799 & 0.3062 & 0.0007 & -1.2465 & 1.5325 & 0 & 1.7000 \\
1.6239 & 0.0087 & 1.7518 & 2.7606 & 0.0010 & -2.6719 & 1.6239 & -0.0067 & 1.7518 \\
1.7328 & 1.6977 & 1.6777 & 2.4660 & 0.0010 & -2.4470 & 1.7329 & 0.0043 & 1.3795 \\
0.3522 & -13.5989 & -0.3284 & 0.8252 & 1.7001 & -1.1535 & 0.9965 & 0.0003 & 0.3327 \\
1.5756 & -8.9389 & 0.0961 & 0.8366 & 1.7002 & -0.9724 & 0.7683 & -0.0075 & 0.7868 \\
0.9694 & -1.6880 & 1.0832 & 2.8336 & 0.0009 & -4.0328 & 0.5291 & 1.6892 & 1.1500 \\
0.6372 & 2.9276 & 0.2250 & 0.0580 & 0.0001 & -2.5327 & 0.9724 & 1.7255 & 0.7105
\end{bmatrix}.$$

thresholds are the upper and lower bounds of the acceptance region $B(k)$ from Eq. (43) with the detection rate λ (the false alarm rate), which means the smaller λ is, the less the false alarms occur.

For the fault-free case, the residuals are same before $t < 4\,\mathrm{sec}.$, in the figures. 7 and 8. In Fig. 7 (fault 1) and Fig. 8 (fault 2), the different detection rates λ are chosen, which leads to the different thresholds. The λ for fault 2 is smaller than that of fault 1, which makes that the area of acceptance region for fault 2 is larger than that of fault 1. From figures. 7 and 8, it can be seen that the residual out of the thresholds of fault 1 is more than that of fault 2, which means that the false alarms of fault 1 is more than that of fault 2. It matches the detection rates λ and υ of these two cases.

In both faults 1 and 2, two amplitudes of faults are chosen: $f_1^0 = 0.2$ and 0.4, $f_2^0 = 0.25$ and 0.45, in which one is smaller than ε_0 from Theorem 2, the other one is larger. In Figs. 7 and 8, it is obvious that when the amplitudes are smaller than ε_0, parts of the residuals are still within the thresholds after faults occur. The fault detection algorithm cannot detect the fault effectively. But for (b) in Figures 7 and 8, the residuals exceed the thresholds to give the valid fault alarms.

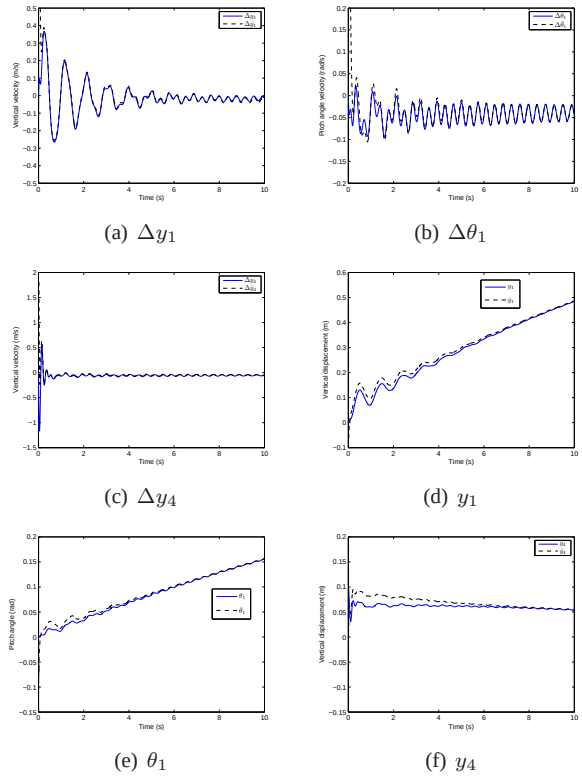

(a) Δy_1 (b) $\Delta\theta_1$ (c) Δy_4 (d) y_1 (e) θ_1 (f) y_4

Fig. 3: States estimates of the first power carbody (showing the designed observing error convergence)

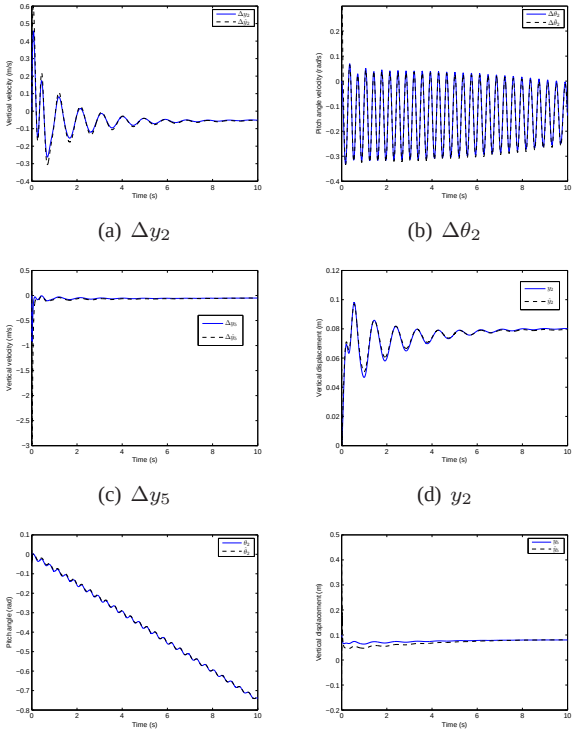

(a) Δy_2 (b) $\Delta\theta_2$ (c) Δy_5 (d) y_2 (e) θ_2 (f) y_5

Fig. 4: State estimates of the trailer carbody (showing the designed observing error convergence)

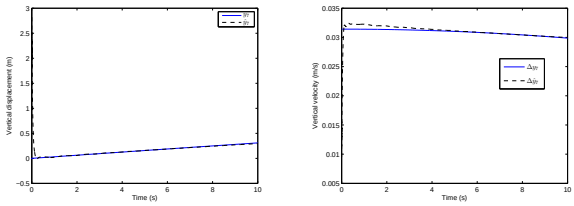

(a) y_7 (b) Δy_7

Fig. 5: The disturbance (track irregularity) estimates of the first power carbody (the estimate error convergence)

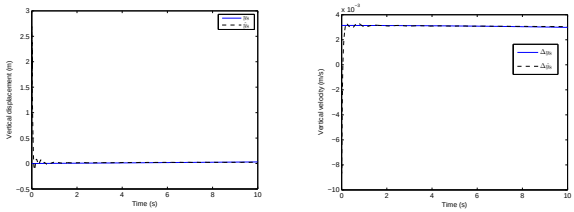

(a) y_8 (b) Δy_8

Fig. 6: The disturbance (track irregularity) estimates of the trailer carbody (the estimate error convergence)

VI. Conclusions

In this paper, the sensor fault detection problem has been investigated for suspension systems with the track regularity and noises, which are modelled as input disturbances with stochastic noise. To design the fault detection observer, the disturbances were augmented to the suspension system states, which leads to a singularity system with stochastic noises. The observer has been designed to generate the fault detection residual. The detection residual is discussed to obtain the fault detection threshold with the fault detectability condition.

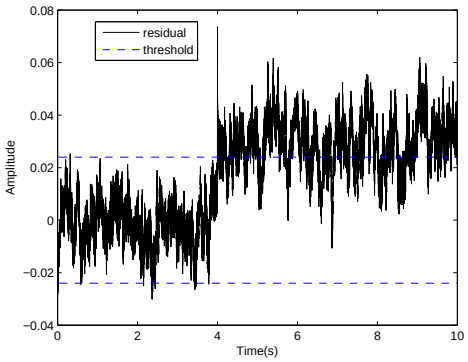

(a) Case of undetectable fault $f_1^0 = 0.2 < \varepsilon_0$

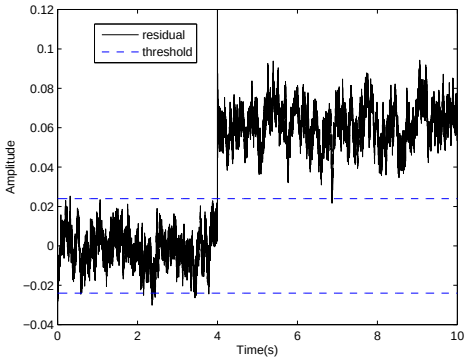

(b) Case of detectable fault $f_1^0 = 0.4 > \varepsilon_0$

Fig. 7: Residual signals and thresholds for noise and fault (see Eq. (50)) with different values of f_1^0.

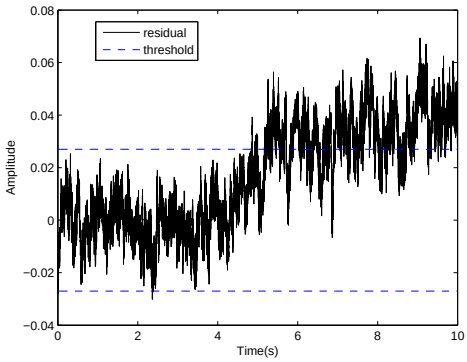

(a) Case of undetectable fault $f_2^0 = 0.25 < \varepsilon_0$

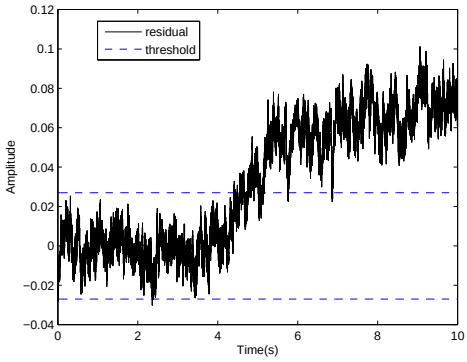

(b) Case of detectable fault $f_2^0 = 0.45 > \varepsilon_0$

Fig. 8: Residual signals and thresholds for noise and fault (see Eq. (51)) with different values of f_2^0.

Simulation results further confirm the obtained theoretical results.

REFERENCES

[1] Y. Lin, C. Lin, N. Shieh, A hybrid evolutionary approach for robust active suspension design of light rail vehicles, *IEEE Transactions on Control System Technology*, vol. 14, no. 4, pp. 695-706, 2006.

[2] H. J. Gao, W. C. Sun, P. Shi, Robust sampled-data H_∞ control for vehicle active suspension systems, *IEEE Transactions on Control Systems Technology*, vol. 18, no. 1, pp. 238-245, 2010.

[3] X. K. Wei, S. Lin and H. Liu, Distributed fault detection observer for rail vehicle suspension systems, *Proc. of Chinese Control and Design Conference*, pp. 3396-3399, 2012.

[4] Z. H. Mao, Y. Wang, B. Jiang, G. Tao, Fault diagnosis for a class of active suspension systems with dynamic actuators faults, *International Journal of Control, Automation, and Systems*, vol. 14, no. 5, pp. 1-13, 2016.

[5] M. Blanke, M. Kinnaert, J. Lunze, M. Staroswiecki, *Diagnosis and fault-tolerant control*, Springer Verlag, Berlin, Heidelberg, 2003.

[6] J. Chen, R. J. Patton, Robust model-based fault diagnosis for dynamic systems, *Kluwer Academic Publishers, London*, 1999.

[7] S. X. Ding, Model-based fault diagnosis techniques, *Springer*, 2013.

[8] X. Zhang, V. Cocquempot, A. Aitouche, Fault-tolerant control scheme based on reference adjustments for a 4WD electric vehicle with actuator faults and constraints, *Proc. of 23th Mediterranean Conference on Control and Automation (MED)*, pp. 218-223, 2015.

[9] W. Chen, W. Chen, M. Saif, M. F. Li, H. Wu, Simultaneous fault isolation and estimation of lithium-ion batteries via synthesized design of Luenberger and learning observers, *IEEE Transactions on Control Systems Technology*, vol. 22, no. 1, pp. 290-298, 2014.

[10] Y. Wang, Y. D. Song, H. Gao, F. L. Lewis, Distributed fault-tolerant control of virtually and physically interconnected systems with application to high-speed trains under traction/braking failures, *IEEE Transactions on Intelligent Transportation Systems*, vol. 17, no. 2, pp. 535-545, 2016.

[11] D. Li, Y. D. Song, D. Huang, H. Chen, Model-independent adaptive fault-tolerant output tracking control of 4WS4WD road vehicles, *IEEE Transactions on Intelligent Transportation Systems*, vol. 14, no. 1, pp. 169-179, 2013.

[12] J. O. Burkholder, G. Tao, Adaptive detection of sensor uncertainties and failures *Journal of Guidance, Control, and Dynamics*, vol. 34, no. 6, pp. 1605-1612, 2011.

[13] Z. H. Mao, B. Jiang, P. Shi, Protocol and fault detection design for nonlinear networked control systems, *IEEE Transactions on Circuits and Systems II: Express Briefs*, vol. 56, no. 3, pp. 255-259, 2009.

[14] H. Zhang, J. M. Wang, Adaptive sliding-mode observer design for a selective catalytic reduction system of ground-vehicle diesel engines, *IEEE/ASME Transactions on Mechatronics*, DOI: 10.1109/TMECH.2016.2542362, 2016.

[15] H. Zhang, G. G. Zhang, J. M. Wang, H_∞ observer design for LPV systems with uncertain measurements on scheduling variables: application to an electric ground vehicle, *IEEE/ASME Transactions on Mechatronics*, vol. 21, no. 3, pp. 1659-1670, 2016.

[16] H. Zhang, G. G. Zhang, J. M. Wang, Sideslip angle estimation of an electric ground vehicle via finite-frequency H_∞ Approach, *IEEE Transactions on Transportation Electrification*, vol. 2, no. 2, pp. 200-209, 2016.

[17] H. J. Yang, Y. Q. Xia, B. Liu, Fault detection for T-S fuzzy discrete systems in finite-frequency domain, *IEEE Transactions on Systems, Man, and Cybernetics, Part B: Cybernetics*, vol. 41, no. 4, pp. 911-920, 2011.

[18] G. H. Yang, H. Wang, Fault detection for a class of uncertain state-feedback control systems, *IEEE Transactions on Control Systems Technology*, vol. 18, no. 1, pp. 201-212, 2010.

[19] X. He, Z. D. Wang, Y. Liu, D. H. Zhou, Least-squares fault detection and diagnosis for networked sensing systems using direct state estimation approach, *IEEE Transactions on Industrial Informatics*, vol. 9, no. 3, pp. 1670-1679, 2013.
[20] B. Jiang, Z. H. Mao, P. Shi, H_∞ filter design for a class of networked control systems via T-S fuzzy model approach, *IEEE Transactions on Fuzzy Systems*, vol. 18, no .1, pp. 201-208, 2010.
[21] M. Chadli, A. Abdob, S. X. Ding, $H\_/H_\infty$ fault detection filter design for discrete-time Takagi-Sugeno fuzzy system, *Automatica*, vol. 49, pp. 1996-2005, 2013.
[22] S. K. Nguang, P. Shi, S. Ding, Fault detection for uncertain fuzzy systems: an LMI approach, *IEEE Transactions on Fuzzy Systems*, vol. 15, no. 6, pp. 1251-1262, 2007.
[23] H. L. Dong, Z. D. Wang, H. J. Gao, Fault detection for Markovian jump systems with sensor saturations and randomly varying nonlinearities, *IEEE Transactions on Circuits and Systems I: Regular Papers*, vol. 59, no. 10, pp. 2354-2362, 2012.
[24] R. Wang, J. M. Wang, Fault-tolerant control with active fault diagnosis for four-wheel independently driven electric ground vehicles, *IEEE Transaction on Vehicle Technology*, vol. 60, no. 9, pp. 4276-4287, 2011.
[25] M. Moradi, A. Fekih, Adaptive PID-sliding-mode fault-tolerant control approach for vehicle suspension systems subject to actuator faults, *IEEE Transaction on Vehicle Technology*, vol. 63, no. 3, pp. 1041-1054, 2014.
[26] X. K. Wei, L. M. Jia, K. Guo, S. Wu, On fault isolation for rail vehicle suspension systems, *Vehicle System Dynamics*, vol. 52, no. 6, pp. 847-873, 2014.

Zehui Mao Zehui Mao received her Ph.D. degree in Control Theory and Control Engineering from Nanjing University of Aeronautics and Astronautics, Nanjing, China, in 2009. She is now an associate professor at the College of Automation Engineering in Nanjing University of Aeronautics and Astronautics, China. she has been a visiting scholar in University of Virginia. She worked in the areas of fault diagnosis, with particular interests in nonlinear control systems, sampled-data systems and networked control systems. Her current research interests include fault diagnosis and fault-tolerant control of systems with disturbance and incipient faults, and high speed train and spacecraft flight control applications.

Yanhao Zhan Yanhao Zhan received his M.S. Degree in Control Engineering from Nanjing University of Aeronautics and Astronautics, Nanjing, China, in 2016. He is now an engineer in CRRC Zhuzhou Institute Co., Ltd, Zhuzhou, China. His research interests include fault diagnosis and fault-tolerant control for high speed train.

Gang Tao Gang Tao (S84 M89 SM 96 F07) received the B.S. degree from the University of Science and Technology of China, Hefei, China, in 1982, and the M.S. and Ph.D. degrees from the University of Southern California, Los Angeles, CA, USA, during 1984-1989. He is currently a Professor at the University of Virginia, Charlottesville, VA, USA. He worked in the areas of adaptive control, with particular interests in adaptive control of systems with multiple inputs and multiple outputs and with nonsmooth nonlinearities and actuator failures, in stability and robustness of adaptive control systems, and in passivity characterizations of control systems. He has authored or coauthored six books, and more than 400 technical papers and book chapters. His current research interests include adaptive control of systems with uncertain actuator failures and nonlinearities, with structural damage and sensor uncertainties and failures, adaptive approximation-based control, and resilient aircraft and spacecraft flight control applications. He has served as an Associate Editor of Automatica, the International Journal of Adaptive Control and Signal Processing, and the IEEE TRANSACTIONS ON AUTOMATIC CONTROL, a Guest Editor of the Journal of Systems Engineering and Electronics, and an Editorial Board Member of the International Journal of Control, Automation and Systems.

Bin Jiang Bin Jiang obtained Ph.D. degree in Automatic Control from Northeastern University, Shenyang, China, in 1995. He had ever been postdoctoral fellow, research fellow and visiting professor in Singapore, France, USA and Canada, respectively. Now he is a Chair Professor of Cheung Kong Scholar Program in Ministry of Education and Dean of College of Automation Engineering in Nanjing University of Aeronautics and Astronautics, China. He currently serves as Associate Editor or Editorial Board Member for a number of journals such as IEEE Trans. On Control Systems Technology; IEEE Trans. On Fuzzy Systems; Int. J. of Control, Automation and Systems; Nonlinear Analysis: Hybrid Systems; Acta Automatica Sinica; Systems Engineering and Electronics Technologies. He is Chair of Control Systems Chapter in IEEE Nanjing Section, a member of IFAC Technical Committee on Fault Detection, Supervision, and Safety of Technical Processes. His research interests include fault diagnosis and fault tolerant control and their applications.

Xing-Gang Yan received the B.Sc. degree of Applied Mathematics from Shaanxi Normal University, in 1985, the M.Sc. degree of Control and Optimisation from Qufu Normal University in 1991, and the Ph.D. degree of Control Engineering from Northeastern University, P. R. China in 1997. Currently, he is appointed as a Senior Lecturer at the University of Kent, United Kingdom. He was a Lecturer in Qingdao University, P. R. China from 1991 to 1994. He worked as a Research Fellow or Research Associate in the Northwestern Polytechnical University, China, the University of Hong Kong, China, Nanyang Technological University, Singapore and the University of Leicester, United Kingdom. He is the Editor-In-Chief of the International Journal of Engineering Research and Science & Technology. He was a lead guest editor for the special issue Advanced Control of Complex Dynamical Systems with Applications in Mathematical Problems in Engineering. He serves as a member of the Editorial Board for several engineering journals. He has published three books, a few book chapters and over 140 referred papers. His research interests include sliding mode control, decentralised control, fault detection and isolation, nonlinear control and time delay systems with applications.